Deactivation of Industrial Pd/Al2O3 Catalysts by Ethanol: A Spectroscopic Study

UNIVERSITÀ DEGLI STUDI DI TORINO

Deactivation of industrial Pd/Al_2O_3 catalysts by ethanol: a spectroscopic study

Michele Carosso,*[a] Eleonora Vottero,[a,b] Sara Morandi,[a] Maela Manzoli,[c] Davide Ferri,[d] Thibault Fovanna,[d] Riccardo Pellegrini,[e] Andrea Piovano,[b] and Elena Groppo[a]

[a] Dr. M. Carosso, Mrs. E. Vottero, Dr. S. Morandi, Prof. E. Groppo
Department of Chemistry, INSTM and NIS Centre
University of Torino
via Quarello 15/A, I-10135 Torino, Italy
E-mail: michele.carosso@unito.it
[b] Mrs. E. Vottero, Dr. A. Piovano
Institut Laue-Langevin (ILL)
71 avenue des Martyrs, F-38000 Grenoble, France
[c] Prof. M. Manzoli
Department of Drug Science and Technology, INSTM and NIS Centre
University of Torino
via Pietro Giuria 9, I-10125 Torino, Italy
[d] Dr. D. Ferri, Dr. T. Fovanna
Paul Scherrer Institut
Forschungsstrasse 111, CH-5232 Villigen PSI, Switzerland
[e] Dr. R. Pellegrini
Chimet SpA - Catalyst Division
via di Pescaiola 74, I-52041, Viciomaggio Arezzo, Italy

Abstract: The chemical processes involved in the decomposition of ethanol over two industrial Pd/Al_2O_3 catalysts characterized by different Pd dispersions, particles morphology and reducibility of the active metal phase was thoroughly investigated in gas-phase and in liquid-phase by transmission FT-IR and ATR-IR spectroscopies, respectively. In both cases, two main products were detected, arising from two competitive paths: acetates from ethanol oxidation and carbonyls from acetaldehyde decarbonylation. The regularity of the Pd particles greatly affects the relative proportion of the two products, while the initial Pd oxidation state influences the kinetics of the two processes. Ethanol oxidation to acetates is the kinetically favored reaction path both in gas-phase and in liquid-phase. In contrast, the presence of a solvent dampens the decarbonylation process to very low levels, because the solvent competes with ethanol in occupying the available surface sites. Since adsorbed carbonyls are considered as surface poisons of industrial Pd/Al_2O_3 catalysts in processes involving aliphatic as well as aromatic alcohols, the rationalization of the experimental variables affecting alcohols decomposition can help in establishing working protocols and in designing preparation procedures that minimize the unwanted poisoning effects.

Introduction

Heterogeneous catalysts based on supported Group VIII metals are widely employed in industrial processes involving hydrogenation of reducible molecular moieties or formation of C-C and C-N chemical bonds, such as in the synthesis of pharmaceuticals and specialty chemicals.[1-4] In the industrial practice, these reactions are carried out in a solvent, such as an aliphatic alcohol.[2-3] However, it has been demonstrated that in some cases alcoholic solvents are not innocuous and lead to a worsening of the catalytic performances.[2-3] As an example, Singh *et al.* documented a five-fold suppression in the rate of cyclohexene reduction when Pd/C was aged for 8-20 h in ethanol, as a consequence of surface poisoning. The same effect was reported for debenzylation reactions and reduction of polar functional groups such as the nitro group.[5]

The occurrence of anaerobic dehydrogenation of alcohols over these metals is a well-known phenomenon, whose reaction pathway was firstly investigated in a series of seminal surface science works. For primary alcohols interacting at 443 °C with a Pd(111) single-crystal surface, Davis and Barteau proposed a decomposition pathway corresponding to the reverse of alcohols synthesis (Scheme 1):[6-7] the alcohol chemisorbs on the metal surface as an alkoxide, which experiences the cleavage of the C-H bond in α position leading to a η^2(O,C)-aldehyde and, by further dehydrogenation, to a η^2(O,C)-acyl species. The adsorbed acyl undergoes decarbonylation, resulting in adsorbed CO, hydrogen and carbonaceous fragments, responsible for the surface poisoning and the subsequent worsening in the catalytic performances. The carbonaceous fragments may react with the adjacent hydrogen species, desorbing as hydrocarbons, or may experience further dehydrogenation leading to an adsorbed carbon phase. Similar findings were reported for Ni(111),[8] Pt(111)[9] and Pd(110),[10] indicating that this mechanism is structure-insensitive. A further confirmation of the involvement of aldehydes and acyl species as intermediates in the anaerobic dehydrogenation of alcohols arises from the observation that when aldehydes are directly contacted with Pd(111) and Pd(110) surfaces, CO, hydrogen and carbonaceous fragments are produced.[11-12]

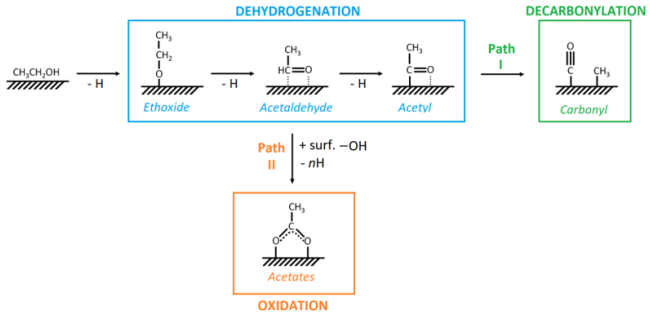

Scheme 1. Schematic representation of the possible decomposition routes for ethanol over Pd/Al_2O_3 catalysts. Ethanol is initially dehydrogenated to give ethoxide and acetaldehyde intermediates. Path I (decarbonylation) involves the complete decomposition of the intermediates, to give carbonyls and carbonaceous fragments. Path II (oxidation) involves the oxidation of the intermediates by surface -OH groups, leading to adsorbed acetates. Both reaction paths require the presence of Pd^0, but the reaction products might be localized also on the alumina support.

Despite their pivotal importance, surface science investigations lack the complexity of real heterogeneous catalysts, where surface chemistry is determined by several parameters such as the morphology and size of the supported metal nanoparticles, the nature of the support and the possible presence of promoters and/or poisons. So far, the reactivity of aliphatic alcohols over Pd-based heterogeneous catalysts was investigated mainly by means of spectroscopic methods. Most of the studies regard methanol and confirm the decomposition pathway proposed on the basis of surface science studies. For example, Solymosi and co-workers reported that gaseous methanol decomposes at room temperature on Pd/SiO_2, giving mostly multi-coordinated carbonyls.[13] Formation of transient formaldehyde was detected by FT-IR spectroscopy. They also found that doping with K adatoms is beneficial in diminishing the surface poisoning by adsorbed CO, stabilizing the intermediates of methanol decomposition. A similar effect was documented by Cabilla *et al.* on unpromoted and Ca-promoted Pd/SiO_2 catalysts.[14] Zecchina and co-workers investigated the Pd-mediated methanol decomposition on Pd/MgO, chlorine-doped Pd/MgO and Pd/Al_2O_3 catalysts.[15] Irrespective of the system, physisorbed methanol and methoxy species chemisorbed at the support were detected, while CO formation was observed at room temperature only on Pd/MgO. Such behaviour was ascribed to the superior basicity of the MgO support.[16] Interestingly, upon increasing the working temperature, formate species were formed on Pd/MgO, indicating the occurrence of an oxidation reaction. Similar evidences for formation of oxidation products in anaerobic conditions were reported for ethanol interacting with a $Pt/CeZrO_2$ bifunctional catalyst[17] and with Pd/CeO_2.[18] Since in all the cases the metal phase was completely reduced, the observation of oxidation products was ascribed to a reaction of the alkoxy species with the -OH groups at the surface of the support (path II in Scheme 1). All in all, these studies indicate that the reactivity of gaseous aliphatic alcohols with Pd-based heterogeneous catalysts depends not only on the Pd phase, but also on the properties of the support (e.g. hydroxylation degree, basicity/acidity, etc.). Moreover, it is clear that CO is always one of the final products of alcohols decomposition over metal surfaces. It is known that CO, due to its very strong adsorption ability, is one of the major poisons for Pd-based catalysts, resulting in the blockage of the available reactive sites and in a subsequent worsening of the catalytic performances when alcohols are used a reaction media. As an example, the presence of adsorbed CO strongly inhibits the alcohols oxidation activity on Pd/Al_2O_3 catalysts.[19-20]

Similar studies were also conducted on not pre-reduced Pd-based heterogeneous catalysts, i.e. where the active phase is initially PdO or surface oxidized Pd. It has been demonstrated that in anaerobic conditions primary alcohols reduce oxidized Pd surfaces, and that the sample reducibility greatly affects the process under investigation.[21] Newton *et al.* hypothesized two reaction routes for ethanol interacting with a PdO phase.[21-22] The alcohol can directly reduce the oxidized metal surface, via an intermediate ethoxide species adsorbed at the PdO phase. The reaction products are Pd^0, acetaldehyde (that can further dehydrogenate on the reduced surface following the previously discussed pathway) and a water molecule. An alternative route forecasts that the reduction of the PdO phase is assisted by gaseous H_2, generated by recombination of adsorbed hydroxyls groups and atomic hydrogen formed upon oxidation of ethanol into acetaldehyde.

The studies discussed above, dealing with reactions occurring at a solid-gas interface, are still over-simplified with respect to industrial conditions, where reactions are carried out in the presence of a solvent and hence occur at a solid-liquid interface. While the characterization for catalytic solid-gas interfaces by FT-IR spectroscopy has reached a very high degree of sophistication,[23-25] much less studies are reported in the literature for heterogeneous catalysts working in a liquid environment,[26] mainly because of technical limitations. Most of the commonly employed organic solvents, as well as water, show absorption bands in spectral regions of interest for elucidating reaction mechanisms, whose intensity can be orders of magnitude stronger than that of the adsorbed surface species. In addition, the large optical path characteristic of transmission cells seriously limits the adoption of FT-IR spectroscopy in transmission for investigating solid-liquid interfaces.[27] On the other hand, attenuated total reflection infrared (ATR-IR) spectroscopy presents a suitable optical geometry for the study of phenomena occurring at solid surfaces immersed in a liquid.[28-32] The oxidation of various alcohols over catalysts immersed in a liquid environment has been the subject of extensive spectroscopic investigation.[33-34] The liquid-phase Pd-mediated dehydrogenation of aliphatic and aromatic alcohols was studied in both anaerobic and aerobic conditions using ATR-IR.[26, 35-38] In the absence of O_2, benzyl alcohol was shown to dehydrogenate into benzaldehyde, which further experiences decarbonylation leading to a CO adlayer that poisons the catalyst surface. Benzoate species were detected also in anaerobic conditions, as a consequence of benzyl alcohol oxidation by some oxygen source (either in the feed and/or at the catalyst surface). The adoption of aerobic conditions enhances the stability of the benzaldehyde intermediate at the expenses of CO formation and favours oxidation to benzoate. It is worth mentioning that electrochemistry tools were also employed to investigate the surface phenomena occurring at the solid-liquid interface of metal electrodes in alkaline liquid media, which are however conditions far from those of interest in catalysis.[39-42]

In this work, we provide an extensive spectroscopic characterization of the ethanol anaerobic dehydrogenation over two industrial Pd/Al_2O_3 catalysts produced by Chimet S.p.A. for hydrogenation of functional groups and debenzylation reactions,

in the field of the production of active pharmaceutical ingredients and fine chemicals. The two catalysts differ in terms of dispersion and reducibility of the Pd phase. Moreover, both gas-phase and liquid-phase protocols have been adopted, in order to bridge the gap of knowledge between the two approaches. The final aim is to provide insights into the preparation and activation variables which have an influence on the ethanol decomposition process, and hence on the catalysts deactivation due to adsorbed CO. The results are useful to select the best synthesis and activation procedures that minimize the surface poisoning effects. It is worth remembering that one of the main drawbacks in adopting infrared spectroscopy as a characterization tool arises from the absorption of spectator species that could overwhelm the signals of the species of interest: while this is particularly relevant for liquid-phase protocols, due to the presence of a bulk solvent, it is not significant for gas-phase protocols, where ethanol is carried out by an inert carrier.

Results and Discussion

Preliminary characterization of the Pd/Al_2O_3 catalysts

The two Pd/Al_2O_3 catalysts under study were already characterized in a previous work by applying a multi-technique approach (including HR-TEM, TPR, SAXS and FT-IR spectroscopy of adsorbed CO),[43] which was devoted to correlate the reduction state of Pd/Al_2O_3 catalysts and their catalytic performance. Hereinafter, the two catalysts will be labeled as PdAl(F) (pre-reduced in liquid-phase with sodium formate) and PdAl (not pre-reduced), following the same nomenclature as in Ref.[44] It was found that in PdAl(F) the surface and sub-surface of the Pd phase was oxidized, but this Pd^{2+} phase is easier to be reduced than the bulk PdO particles present in PdAl. Moreover, the two catalysts displayed a different Pd dispersion, D(%), as evaluated by CO chemisorption, namely D = 24% for PdAl(F) and D = 36% for PdAl. The lower Pd dispersion in PdAl(F) was ascribed to a greater interaction of the Pd nanoparticles with the support and a slightly larger particle size. Once reduced in H_2, the Pd nanoparticles in PdAl(F) exhibited a larger fraction of sites located on extended surfaces, while those in PdAl were more irregular and displayed a larger fraction of edges and corners. Analysis of SAXS data revealed for PdAl an average particle size centered around 1.5 nm. PdAl(F) has a similar value, but its size distribution is characterized by a tail towards greater values, that explains the lower dispersion.[43]

Reactivity of gaseous ethanol over Al_2O_3 and Pd/Al_2O_3 catalysts: assignment of the main IR absorption bands

Before investigating the interaction of ethanol with the Pd/Al_2O_3 catalysts, we considered its adsorption on the bare Al_2O_3 support. Figure 1a shows the FT-IR spectra of Al_2O_3 (activated at 120 °C in a N_2 stream for 30 min) before (spectrum 1, black) and after ethanol exposure (spectrum 2, blue), while Figure 1c reports the difference between the two spectra (spectrum 2, blue) compared with that of gaseous ethanol (spectrum 1, grey) in the 2200-1200 cm^{-1} region. The FT-IR spectrum of Al_2O_3 activated at 120 °C is dominated by the ν(OH) stretching modes of the surface hydroxyl groups showing a different degree of hydrogen-bonding (bands in the 3800-3000 cm^{-1} range) and by the framework modes of Al_2O_3 (below 1000 cm^{-1}). Upon exposure of Al_2O_3 to ethanol at room temperature, the vibrational features of gaseous and physisorbed ethanol appeared immediately. The most intense bands are observed in the 3000-2800 cm^{-1} range (ν(CH_x) stretching modes) and at ca. 1050 cm^{-1} (ν(C-O) stretching mode) (Figure 1a). In the 1500-1200 cm^{-1} range (Figure 1c) the weak bands at ca. 1490 (δ(CH_2) mode), 1452 ($\delta_{asym}(CH_3)$), 1394 ($\delta_{sym}(CH_3)$) and 1242 cm^{-1} (δ(OH)) are ascribed to gaseous ethanol (spectrum 1, grey), while those (more intense) at 1485, 1450, 1385 and 1242 cm^{-1} are assigned to the same vibrational modes of physisorbed ethanol (spectrum 2, blue). At the same time, the broad band due to the hydroxyl groups of the Al_2O_3 surface was affected by the presence of ethanol. In particular, the shoulder of isolated -OH species at ca. 3720 cm^{-1} was consumed in favor of a more pronounced band at ca. 3500 cm^{-1}, testifying the occurrence of a hydrogen-bonding interaction between the Al_2O_3 surface and physisorbed ethanol. It is worth noticing that the presence of physisorbed ethanol does not allow to discriminate chemisorbed ethoxy species possibly formed upon reaction of ethanol with surface -OH species, as previously documented for Al_2O_3 as well as for other supports.[13-14]

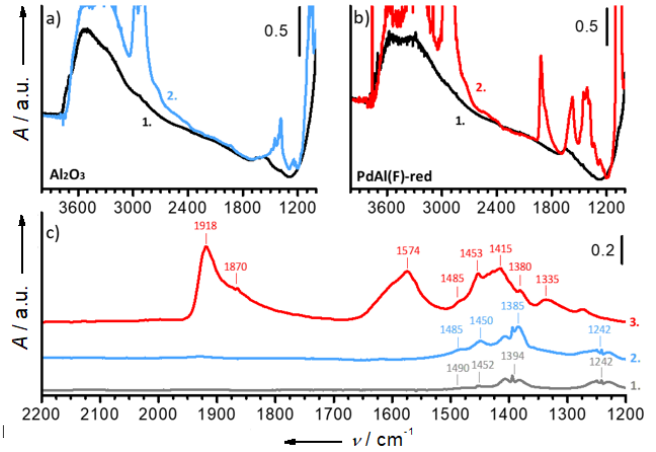

and of the same sample exposed to ethanol at room temperature for 30 min (spectrum 2, blue). Part b): FT-IR spectra of PdAl(F)-red (spectrum 1, black) and of the same sample after a prolonged exposure to ethanol at room temperature (spectrum 2, red). Part c): difference between the two spectra reported in part a) (spectrum 2, blue) and part b) (spectrum 3, red), compared to the spectrum of gaseous ethanol (spectrum 1, grey), in the 2200–1200 cm^{-1} region.

The same experiment was repeated on the two Pd/Al_2O_3 catalysts activated according to the two protocols described in the experimental section. The reaction products were the same in the four experiments, although their relative amount and the kinetics of their formation were different from case to case, as it will be discussed in the following section. Herein, we start discussing the main reaction products and their spectroscopic features, taking the PdAl(F)-red catalyst as an example. Figure 1b shows the FT-IR spectra of activated PdAl(F)-red before (spectrum 1, black) and after ethanol exposure (spectrum 2, red), while Figure 1c reports the difference between the two spectra (spectrum 3, red). The spectrum of the activated catalyst is almost indistinguishable from that of activated Al_2O_3 (Figure 1a). After interaction with ethanol (up to 100 min), the absorption bands of gaseous and

physisorbed ethanol are well visible. Moreover, very intense bands appeared in the 2200–1200 cm^{-1} region, which were not present in the case of bare Al_2O_3 (compare blue and red spectra in Figure 1c). These bands are assigned to two products of the ethanol reaction with the catalyst.

The bands at 1918 and 1870 cm^{-1} belong to 2-fold bridged carbonyls at Pd(100) and 3-fold carbonyls in hollow sites at Pd(111) surfaces, respectively. Bands in similar position have been reported for CO adsorbed on Pd single crystals,[45-46] and on Pd nanoparticles,[16, 47-48] at low CO coverages. The observation of these bands indicates the occurrence of the decarbonylation path on PdAl(F)-red. The bands at 1574 (vs) and 1415 (vs) cm^{-1} are assigned to the ν_{as}(COO) and ν_s(COO) modes of acetate species, respectively, whose $\delta(CH_3)$ mode is overlapped to those of physisorbed ethanol. The position of the ν(COO) bands indicates that the acetates are adsorbed in a bridged geometry.[49] Adsorbed acetates must derive from the oxidation of acetaldehyde, the product of ethanol dehydrogenation.[15, 17-18, 36, 40-41] Since the Pd phase in the PdAl(F)-red catalyst was completely reduced, the most likely oxidant species are the hydroxyl groups at the Al_2O_3 surface, as suggested previously.[13-14, 17-18] As far as the location of the acetates is concerned, they might be at the surface of both Al_2O_3 and Pd. However, their absence when ethanol was dosed on bare Al_2O_3 encourages us to conclude that their formation requires the presence of Pd. Hence, our data suggest a close cooperation between the Pd nanoparticles and the Al_2O_3 support in the formation of the acetate species. Pd is necessary to dehydrogenate ethanol into acetaldehyde, while further oxidation is supported by the only available oxidant source, the hydroxyl groups of the support. These hydroxyls located at the metal-support interface are those most likely involved, being the closest to the dehydrogenation product.

Ethanol decomposition over PdAl(F) and PdAl: reaction by-products and their formation kinetics

Figure 2 reports the whole sequences of FT-IR spectra collected during the prolonged treatment in ethanol for the two catalysts activated according to the two different protocols described in the experimental section. As anticipated above, regardless of the sample and of the activation protocol, the same decomposition products were observed (namely, carbonyls and acetates), although the kinetics of their formation and their relative concentration differed from sample to sample.

In all the experiments, except for PdAl-ox, the bands assigned to acetates appeared almost immediately, and reached their maximum intensity within 3 min. This is particularly evident for the ν_{as}(COO) mode at 1574 cm^{-1} (as shown in Figure 3, which reports the evolution of the band intensity as a function of time), while the ν_s(COO) mode at 1415 cm^{-1} overlapped with the bands of physisorbed ethanol that increased constantly along the whole experiment. This observation suggests that the oxidation of ethanol to acetates is kinetically favored, but also that the oxidant species are rapidly consumed. Such consideration, together with the experimental evidence of the absence of acetate species when ethanol interacts with the bare Al_2O_3 support, confirms that ethanol oxidation is mediated by the Pd phase and that the most likely oxidant species are the –OH groups located at the metal-support interface. On PdAl-ox (Figure 2d) the bands due to acetates appeared at a much lower rate, and reached their maximum intensity after more than 1 h (Figure 3d). Such behavior is in agreement with previous findings indicating that, despite the role of the -OH groups at the Al_2O_3 surface as oxidants, Pd^0 is necessary for catalyzing ethanol oxidation through dehydrogenation. In this sample, Pd is initially entirely in the form of PdO, which needs to be reduced to Pd^0 by ethanol (which is oxidized to acetaldehyde) for initiating its catalytic activity, thus explaining the delay in the appearance of the absorption bands of acetates.

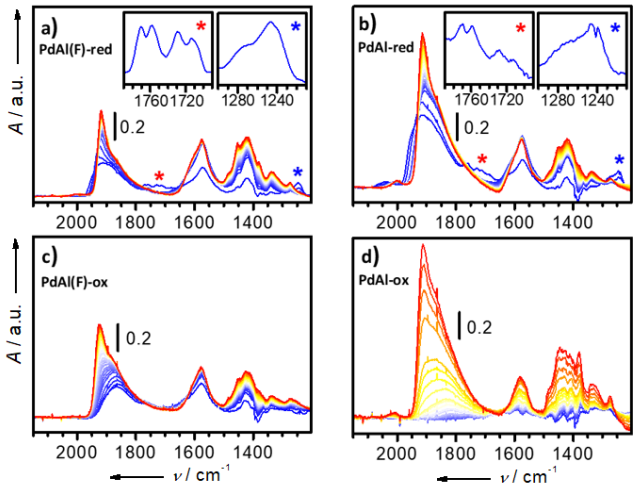

Figure 2. FT-IR spectra collected during the exposure of the PdAl(F) and PdAl catalysts to ethanol at room temperature. All the spectra are shown after subtraction of the spectrum of the catalyst prior the exposure to ethanol. Samples were activated following the two different protocols described in the experimental section (red and ox), Insets in parts a) and b) show a magnification of the signals labelled with an asterisk.

Besides the appearance of the acetate bands, as soon as ethanol reached the reduced catalysts two weak transient bands were observed at ca. 1730 and 1250 cm^{-1} (asterisks in Figure 2a and Figure 2b, magnified in the insets), which disappeared after 5 min. Their transient character suggests an attribution to labile intermediates. More in detail, the broad and weak feature at 1730 cm^{-1} is composed of two pairs of bands centered at 1770 and 1758 cm^{-1} and at 1729 and 1713 cm^{-1}. The latter pair is ascribed to gaseous acetaldehyde (ν(C=O)), formed as a labile intermediate in ethanol dehydrogenation according to Scheme 1. The pair of bands at 1770 and 1758 cm^{-1} and the band at 1250 cm^{-1} are assigned to ethyl acetate (ν(C=O) and ν(C-C-O) respectively).[50] Ethyl acetate is likely formed through the Al_2O_3-catalyzed Tishchenko reaction,[51] which consists in a proton transfer between two adsorbed acetaldehyde molecules. The net result is the formation of an acetate species in the proximity of an ethoxide: the two species quickly react with each other, via esterification. In the experiments performed on the oxidized catalysts these species are not detected, likely because acetaldehyde is rapidly oxidized by PdO before reacting with the Al_2O_3 surface.

The absorption bands of palladium carbonyls increased at different rates in the four experiments and were characterized by different intensities. Figure 3 shows the evolution of the intensity of the bands at 1918 cm^{-1} (2-fold carbonyls at Pd(100), full line) and 1870 cm^{-1} (3-fold carbonyls at Pd(111), dotted line) along the course of the experiments during ethanol exposure. In all the

cases, the band at 1870 cm^{-1} saturated first, indicating that the 3-fold hollow sites at the Pd(111) surfaces are more rapidly filled by CO. On the contrary, the band at 1918 cm^{-1} increased initially fast and then slower along the experiment, indicating that the Pd nanoparticles are not saturated by CO and that decarbonylation progresses slowly with time. Regardless of the sample and/or activation protocol, the formation of acetates is kinetically favored over carbonyls, reflecting the ready availability of the oxidant species (the -OH groups at the Al_2O_3 support), as shown in Figure 3 (black line).

The two reduced catalysts (Figure 3a and b) exhibited a similar behavior. However, the spectra of PdAl-red displayed almost a double intensity compared to those of PdAl(F)-red along the whole experiment. On the other hand, comparison of PdAl(F)-red and PdAl(F)-ox (Figure 3a and c) demonstrates different kinetics, carbonyls appearing at a slower rate in the case of PdAl(F)-ox. This is particularly evident for the absorption band at 1918 cm^{-1} that, for the first 20 min, was less intense than that at 1870 cm^{-1}. However, after 100 min of reaction, the intensity of both bands was almost the same in the two experiments. This behavior is enhanced in the case of PdAl-ox (Figure 3d), where the bands at 1918 and 1870 cm^{-1} started to appear only after about 20 min of reaction. However, also in this case, after 100 min the intensity of both bands was almost the same as that observed during the experiment on PdAl-red (Figure 3b). The delay in the appearance of the carbonyls in the experiments performed on the two oxidized catalysts is explained again by considering that Pd^0 is necessary for catalyzing the decarbonylation, and consequently this process can only begin after the reduction of PdO by ethanol. This process is very slow on PdAl-ox because only in this sample the palladium phase was initially entirely in the PdO form. On PdAl(F)-ox instead the activation in air forms an outer layer of PdO, which is quickly reduced by ethanol.

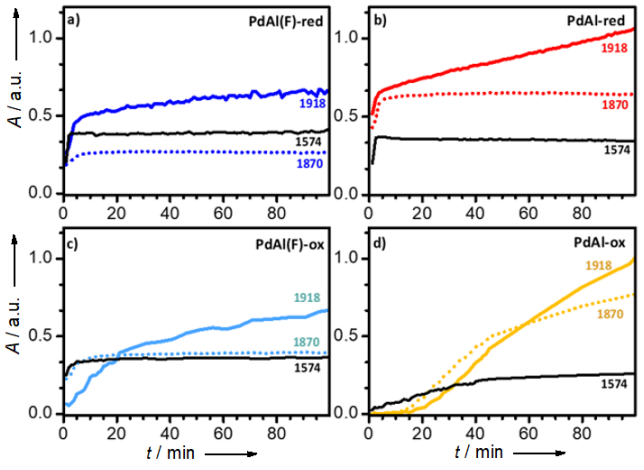

Figure 3. Temporal dependence of the absorption bands at 1918 cm^{-1} (2-fold carbonyls at Pd(100), full line) and 1870 cm^{-1} (3-fold carbonyls at Pd(111), dotted line) ascribed to adsorbed CO, and at 1574 cm^{-1} (black line) ascribed to adsorbed acetates.

Figure 4 compares the ν(CO) region of the spectra collected after 2 min (Figure 4a) and 100 min (Figure 4b) of exposure of the catalysts to ethanol in the four experiments. The first important

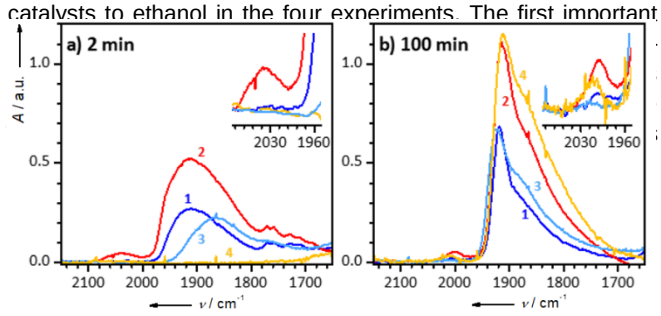

reported in the literature for supported Pd NPs, linear carbonyls form only at high CO coverages, when the molecules are forced in the top position due to compression effects.[16]

As already commented above, both at the beginning and at the end of the experiment, the intensity of the carbonyl bands of PdAl-red is almost double compared to that of PdAl(F)-red, indicating that a larger amount of carbonyls is formed on the former. The spectra collected at the beginning of the experiment on PdAl(F)-red and PdAl-red (spectra 1 and 2, Figure 4a) are very similar. They are dominated by a very broad band, which is the result of the overlap of the two components at 1918 and 1870 cm^{-1} with an additional band at ca. 1950 cm^{-1}. The latter band is also ascribed to 2-fold carbonyls coordinated to Pd(100), but for higher CO coverage. This band disappears after a few minutes of reaction, as a result of the competition between CO and ethanol for the occupancy of the same surface sites, which causes a decrease of the overall CO coverage. Moreover, in the spectrum of PdAl-red a weak band is also observed at 2040 cm^{-1} (inset of Figure 4a), which is assigned to a small fraction of linear carbonyls. The low frequency of this band is explained by considering that the linear carbonyls are perturbed by the presence of other adsorbed species nearby (such as physisorbed ethanol, ethoxy, methyl, etc.).

The spectra collected at the end of the experiment (spectra 1 and 2, Figure 4b) are also very similar and are dominated by the band at 1918 cm^{-1} due to 2-fold bridged carbonyls on Pd(100). In both cases, a weak band is observed at ca. 2000 cm^{-1} (inset of Figure 4b) revealing the presence of a few linear carbonyls. It is interesting to note that this band is red-shifted by ca. 40 cm^{-1} with respect to the beginning of the experiment (inset of Figure 4a). We assign this shift to the interaction of adsorbed CO with a larger amount of adsorbed species, which results in a very low net CO coverage where all the adsorbed carbonyls are “isolated”.

In the case of PdAl(F)-ox, where the kinetics of carbonyls formation is slightly slower than on PdAl(F)-red, the initial spectrum (spectrum 3, Figure 4a) shows only the band at 1870 cm^{-1}. Hence, the 3-fold hollow sites at the Pd(111) surface are the very first ones to be occupied as soon as CO is formed in the reaction. This view is in accordance with the evidence by Ferri and co-workers that benzyl alcohol decomposition to CO preferentially occurs on hollow sites located at (111) facets, while the preliminary dehydrogenation step (aldehyde formation) occurs on (100) facets.[35] In marked contrast, the spectrum collected after 100 min of reaction (spectrum 3, Figure 4b) is very similar to that of PdAl(F)-red (spectrum 1, Figure 4b), in terms of both intensity and band position. The main difference is the position of the weak band assigned to linear carbonyls, which is observed at 2015 cm^{-1} for PdAl(F)-ox and at 2000 cm^{-1} for PdAl(F)-red (inset of Figure 4b). Finally, no carbonyls are observed on PdAl-ox after 2 min of exposure to ethanol (spectrum 4, Figure 4a), while at the end of the experiment (spectrum 4, Figure 4b) the spectrum is very similar to that collected on PdAl-red (spectrum 2, Figure 4b), except for the small shift in the position of the band ascribed to linear carbonyls (inset of Figure 4b).

Figure 4. FT-IR spectra, in the v(CO) region, collected after 2 min (part a) and 100 min (part b) of catalysts exposure to the N_2/ethanol flow. In both parts, the labels are as following: 1 = PdAl(F)-red; 2 = PdAl-red; 3 = PdAl(F)-ox; 4 = PdAl-ox. The insets show a magnification of the 2100–1950 cm^{-1} region. All the spectra are shown after subtraction of the spectrum of the catalyst prior to ethanol exposure.

Altogether, the data reported in Figure 3 and Figure 4 demonstrate that ethanol undergoes decomposition to CO on both PdAl(F) and PdAl catalysts. The oxidation state of the Pd phase (which is tuned through the activation treatment, i.e. reduction vs. oxidation) does not affect the result of exposure to ethanol: after 100 min in the same reaction conditions, the amount and the type of carbonyls are the same on PdAl(F)-red and PdAl(F)-ox as well as on PdAl-red and PdAl-ox. However, the oxidation state of Pd strongly influences the kinetics of the decarbonylation: the more oxidized the Pd phase, the slower the reaction. The size and the surface regularity of the Pd particles, instead, have an effect on the efficiency of the decarbonylation. Irrespective of the kinetics, after 100 min of reaction the amount of carbonyls formed on PdAl is on average twice that observed on PdAl(F). This is not only due to the higher dispersion of PdAl than PdAl(F). According to our previous work,[43] the ratio between the intensity of bands of CO adsorbed at room temperature on PdAl and PdAl(F) is only 1.4. Hence, we can conclude that carbonyls formation is favored on the small and defective Pd nanoparticles present on PdAl rather than on the large and regular ones observed on PdAl(F).

Effect of the liquid environment on ethanol decomposition

For the industrial applications of the catalysts, their interaction with liquid ethanol should be considered. However, the investigation of the phenomena occurring at a solid-liquid interface is complicated by the presence of the bulk liquid phase. For this reason, it is a common academic practice to dilute the considered solvent molecule in another one, that is innocuous toward the system and whenever possible toward spectroscopy. In the present case, we investigated the decomposition of ethanol on the H_2-reduced PdAl(F) catalyst using a 10 mM ethanol solution in cyclohexane. The rather low concentration of ethanol was selected in order to allow for a kinetically controlled formation of the surface species arising from ethanol decomposition over the Pd phase. The ethanol/cyclohexane solution can be considered as a model of what the chemistry that occurs in the presence of pure ethanol, that is the situation more common in industrial applications.

The ATR-IR spectra collected during exposure of the PdAl(F)-red catalyst to the ethanol/cyclohexane solution are reported in Figure 5a. Ideally, the experiment is equivalent to that reported in Figure 2a, except that the H_2-reduction step is conducted at 70 °C (instead of 120 °C) and the solvent is present. The decomposition products observed during the experiment are essentially the same as in the gas-phase experiments, namely acetates and Pd-carbonyls. However, in the presence of the solvent, a single carbonyl band is observed at 1845 cm^{-1}, which is weak and red-shifted with respect to those observed in the gas-phase experiment. The band is assigned to 3-fold carbonyls adsorbed at hollow sites on Pd(111) facets. Both position and intensity indicate that the CO coverage is much lower when ethanol reaches the catalyst in the presence of the cyclohexane solvent than in the gas-phase. The intensity ratio between acetate and Pd-carbonyl signals is in favor of the former species, while Pd-carbonyls dominate in the gas-phase experiments. While this can be certainly attributed also to the low concentration of ethanol in the ATR-IR experiment compared to the ethanol partial pressure in the gas-phase, we consider as well that the cyclohexane solvent competes for the occupancy of the adsorption sites on the Pd nanoparticles responsible for ethanol decomposition, preventing at least partially the decarbonylation. This effect could even be enhanced by the presence of reduced metal because of a potentially stronger Pd-cyclohexane interaction compared to PdO.

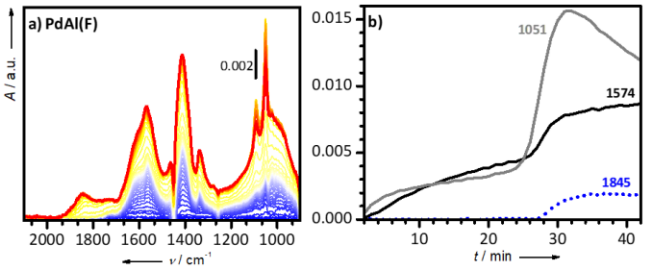

Figure 5. Part a): ATR-IR spectra collected during the exposure of H_2-reduced PdAl(F) catalyst to a 10 mM ethanol solution in cyclohexane at room temperature. All the spectra were recorded after collecting a background prior to the dosage of the ethanol containing solution. Part b): Temporal dependence of the absorption bands at 1845 cm^{-1} ascribed to adsorbed CO, at 1574 cm^{-1} ascribed to adsorbed acetates, and at 1051 cm^{-1} due to physisorbed ethanol.

Figure 5b shows the evolution of the intensity of the bands at 1574 cm^{-1} (ν_{as}(COO) of acetates), 1845 cm^{-1} (3-fold carbonyls at Pd(111), dotted line) and 1051 cm^{-1} (ν(C-O) of physisorbed ethanol) along the course of the experiment. Comparison with Figure 3 reveals that the kinetics are much slower than in the gas-phase, which can be attributed again to the very low ethanol concentration in the liquid medium (10 mM), at least partly. The three signals experience an intensity jump at about 25 min after introduction of ethanol, but it is clear that ethanol was converted to acetate species before this event. We attribute this behavior to the poor solubility of ethanol in cyclohexane at ambient temperature and hence to its low diffusion within the liquid medium.[52] The sudden increase in intensity is likely due to the arrival at the catalyst surface of a "drop" of solvent particularly rich in ethanol, as the following intensity decrease of the signal at 1051 cm^{-1} suggests. This accelerates both ethanol decomposition and oxidation pathways. As observed in the gas-phase, formation of acetates (i.e. the oxidation route) is kinetically favored over decarbonylation. However, the presence of the solvent has the effect of lowering the surface poisoning effects induced by adsorbed CO species, with a pronounced preference towards ethanol oxidation.

Conclusion

In this work we provided a comprehensive characterization of the potentially poisoning phenomena occurring at the surface of two industrial Pd/Al_2O_3 catalysts exhibiting different size and surface regularity of the Pd nanoparticles using *operando* FT-IR and ATR-IR spectroscopy. The two catalysts were activated following two different protocols in order to tune the oxidation state of Pd. We confirmed that ethanol decomposes following two parallel paths: it is rapidly oxidized to acetates and it is slowly dehydrogenated to acetaldehyde (detected as a labile intermediate together with ethyl acetate), which further decarbonylates to give Pd carbonyls.

In gas-phase, oxidation is very fast when the Pd phase is reduced, but it stops as soon as the oxidant species (i.e. the -OH groups at the Al_2O_3 surface) are consumed. When Pd is partially or completely oxidized, the reaction is slower, because ethanol must first reduce PdO to Pd^0. Ethanol dehydrogenation and subsequent acetaldehyde decarbonylation proceed with slower kinetics than ethanol oxidation. These reactions continue accumulating surface species, thus bearing the potential to poison Pd/Al_2O_3 for prolonged exposure, with the consequent worsening of the catalytic performances. At long reaction times, the extent of decarbonylation does not depend on the oxidation state of Pd, but it is strongly affected by the size and the surface regularity of the Pd particles: in the same experimental conditions, smaller and irregular Pd particles decompose ethanol to a larger extent compared to larger and more regular ones. The oxidation state of Pd, instead, plays a role in the kinetics of ethanol dehydrogenation, the more oxidized the Pd phase, the slower the reaction. Ethanol oxidation to acetates remains the kinetically favored reaction path also in liquid-phase. In contrast, the decarbonylation process is dampened to very low levels, because the solvent competes with ethanol in occupying the available surface sites.

Although most of the spectroscopic data presented in this work have been collected in conditions far from those adopted industrially, they provide important information to rationalize how different variables affect ethanol decomposition on industrial Pd/Al_2O_3 catalysts used in liquid-phase catalyzed reactions, helping in establishing working protocols and in designing preparation procedures that minimize the unwanted poisoning effects. According to our results, when working with ethanol as a solvent, it is preferable to employ catalysts having a lower Pd dispersion and with the Pd phase in the oxidized state. Ethanol decomposition cannot be avoided, but it will be delayed and it will be less efficient than that occurring on catalysts with a higher Pd dispersion and with the Pd phase in the reduced state.

Experimental Section

Catalysts synthesis

Two industrial 5 wt% Pd/Al_2O_3 catalysts (provided by Chimet S.p.A.) were prepared from a commercial high-surface-area transition alumina as the support (specific surface area, 116 $m^2 \cdot g^{-1}$; pore volume, 0.41 $cm^3 \cdot g^{-1}$) following a deposition-precipitation using Na_2PdCl_4 as the metal precursor and Na_2CO_3 as the basic agent as described elsewhere.[43-44, 53-54] Both catalysts were carefully washed with water until complete removal of chlorine residues and kept in the wet state (ca. 50 wt% water) until the measurements. In one case, after Pd deposition and before Cl^- removal, the catalyst was pre-reduced in liquid-phase using sodium formate at 65 °C for 1 h.

Methods

Gas-phase operando FT-IR spectroscopy

For the *operando* FT-IR measurements, ca. 10 mg of each catalyst were pressed into self-supported pellets and placed inside a commercial FT-IR reactor cell (AABSPEC, no. 2000-A multimode), which allows recording spectra under controlled temperature and gas atmosphere. The FT-IR spectra were recorded in transmission mode at a resolution of 2 cm^{-1} on a PerkinElmer System 2000 spectrophotometer equipped with a MCT detector.

The samples were activated directly inside the cell. Two activation protocols (for the reduction and the oxidation of the catalyst, respectively) were adopted consisting in three equivalent subsequent steps except for the gas used in step 2. 1) The catalysts were heated to 120 °C (heating rate 2.5 °C/min) under a N_2 flow (50 mL/min) and left at this temperature for 30 min in order to eliminate most of the physisorbed water; then, 2) they were treated in a pure H_2 (or air) flow (50 mL/min) for 30 min; finally, 3) they were quickly cooled to room temperature in flowing N_2 (50 mL/min). The catalyst labels are therefore followed by -red if they have been treated in H_2 or by -ox if they have been treated in air. Hence, four cases are discussed: PdAl(F)-red, PdAl-red, PdAl(F)-ox and PdAl-ox. In the first two cases, the Pd nanoparticles are expected to be completely reduced to Pd^0.

After activation, a spectrum of the catalyst was collected before ethanol was dosed at room temperature by flowing N_2 (50 mL/min) through an ethanol-filled saturator, and spectra were recorded every minute for the first 10 min, then every 2 min up to 20 min, and finally every 5 min for a total of 100 min of exposure.

Liquid-phase operando ATR-IR spectroscopy

For the *operando* ATR-IR experiments, a slurry of the PdAl(F) powder catalyst (ca. 10 mg) in milli-Q water (1 mL) was dropped on a ZnSe internal reflection element (IRE; 52x20x2 mm) and was dried overnight in a fume hood. The dried catalyst layer was then inserted into a home-made ATR-IR cell working in continuous flow and whose temperature is regulated using a recirculating water bath. Cyclohexane was selected as the solvent, because it does not exhibit absorptions in the spectral region of interest and allows us working at relatively high temperature (70 °C). All the measurements were performed employing a Bruker Vertex70 spectrophotometer equipped with a MCT detector and a commercial mirror unit. The ATR-IR spectra were collected at 4 cm^{-1} resolution in the 4000-500 cm^{-1} range.

H_2-saturated cyclohexane was continuously pumped over the catalyst layer during the activation procedure at 70 °C using a peristaltic pump (Ismatec). In order to compensate for the spectral features of the IRE, of the sample and of cyclohexane, a background was collected immediately prior to the dosage of the ethanol solution. Then, an Ar-saturated ethanol solution (10 mM) in cyclohexane was introduced in the cell at room temperature,

and spectra were collected every minute until no spectral changes occurred.

Keywords: Pd/Al_2O_3 catalysts • Alcohol • Poisoning • Gas-phase FT-IR spectroscopy • Liquid-phase ATR-IR spectroscopy

[1] R. L. Augustine in *Heterogeneous Catalysis for the Synthetic Chemist*, Dekker, New York (N.Y.), **1995**, pp. 640.
[2] G. M. Loudon in *Organic Chemistry. 2nd Ed*, Benjamin/Cummings Pub. Co., Menlo Park (CA), **1988**, pp. 1259.
[3] S. Nishimura in *Handbook of Heterogeneous Catalytic Hydrogenation for Organic Synthesis*, Wiley, Weinheim, **2001**, pp. 784.
[4] P. N. Rylander in *Best Synthetic Methods: Hydrogenation Methods*, Academic Press, **1985**, pp. 19
[5] U. K. Singh, S. W. Krska, Y. Sun, *Org. Process Res. Dev.* **2006**, *10*, 1153-1156.
[6] J. L. Davis, M. A. Barteau, *Surf. Sci.* **1987**, *187*, 387-406.
[7] J. L. Davis, M. A. Barteau, *Surf. Sci.* **1990**, *235*, 235-248.
[8] S. M. Gates, J. N. Russell, J. T. Yates, *Surf. Sci.* **1986**, *171*, 111-134.
[9] B. A. Sexton, K. D. Rendulic, A. E. Huges, *Surf. Sci.* **1982**, *121*, 181-198.
[10] R. Shekhar, M. A. Barteau, *Catal. Lett.* **1995**, *31*, 221-237.
[11] J. L. Davis, M. A. Barteau, *J. Am. Chem. Soc.* **1989**, *111*, 1782-1792.
[12] R. Shekhar, M. A. Barteau, R. V. Plank, J. M. Vohs, *J. Phys. Chem. B* **1997**, *101*, 7939-7951.
[13] J. Raskó, J. Bontovics, F. Solymosi, *J. Catal.* **1994**, *146*, 22-33.
[14] G. C. Cabilla, A. L. Bonivardi, M. A. Baltanás, *J. Catal.* **2001**, *201*, 213-220.
[15] S. Bertarione, D. Scarano, A. Zecchina, V. Johanek, J. Hoffmann, S. Schauermann, J. Libuda, G. Rupprechter, H.-J. Freund, *J. Catal.* **2004**, *223*, 64-73.
[16] S. Bertarione, D. Scarano, A. Zecchina, V. Johánek, J. Hoffmann, S. Schauermann, M. M. Frank, J. Libuda, G. Rupprechter, H.-J. Freund, *J. Phys. Chem. B* **2004**, *108*, 3603-3613.
[17] S. M. De Lima, A. M. Silva, U. M. Graham, G. Jacobs, B. H. Davis, L. V. Mattos, F. B. Noronha, *Appl. Catal. A Gen.* **2009**, *352*, 95-113.
[18] A. Yee, S. J. Morrison, H. Idriss, *J. Catal.* **1999**, *186*, 279-295.
[19] J. Wang, G. Aguilar-Rios, R. Wang, *Appl. Surf. Sci.* **1999**, *147*, 44-51
[20] C. Keresszegi, T. Bürgi, T. Mallat, A. Baiker, *J. Catal.* **2002**, *211*, 244-251
[21] J. B. Brazier, B. N. Nguyen, L. A. Adrio, E. M. Barreiro, W. P. Leong, M. A. Newton, S. J. A. Figueroa, K. Hellgardt, K. K. M. Hii, *Catal. Today* **2014**, *229*, 95-103.
[22] M. A. Newton, J. B. Brazier, E. M. Barreiro, S. Parry, H. Emmerich, L. A. Adrio, C. J. Mulligan, K. Hellgardt, K. K. Hii, *Green Chem.* **2016**, *18*, 406-411.
[23] C. Lamberti, E. Groppo, G. Spoto, S. Bordiga, A. Zecchina in *Infrared Spectroscopy of Transient Surface Species*, Vol. 51 (Eds: B. C. Gates,H. Knözinger), Academic Press, **2007**, pp 1-74.
[24] G. Rupprechter in *Sum Frequency Generation and Polarization–Modulation Infrared Reflection Absorption Spectroscopy of Functioning Model Catalysts from Ultrahigh Vacuum to Ambient Pressure*, Vol. 51 (Eds: B. C. Gates,H. Knözinger), Academic Press, **2007**, pp 133-263.
[25] N.-Y. Topsøe, *Catal. Today* **2006**, *113*, 58-64.
[26] D. Ferri, A. Baiker, *Top. Catal.* **2009**, *52*, 1323-1333.
[27] C. H. Rochester, *Adv. Colloid Interface Sci.* **1980**, *12*, 43-82.
[28] T. Bürgi, R. Wirz, A. Baiker, *J. Phys. Chem. B* **2003**, *107*, 6774-6781.
[29] G. M. Hamminga, G. Mul, J. A. Moulijn, *Chem. Eng. Sci.* **2004**, *59*, 5479-5485.
[30] A. Pintar, R. Malacea, C. Pinel, G. Fogassy, M. Besson, *Appl. Catal. A Gen.* **2004**, *264*, 1-12.
[31] J. E. Rekoske, M. A. Barteau, *Ind. Eng. Chem. Res.* **1995**, *34*, 2931-2939.
[32] Z. Wang, M. L. Larsson, M. Grahn, A. Holmgren, J. Hedlund, *Chem. Commun. (Cambridge, U. K.)* **2004**, 2888-2889.
[33] J.-D. Grunwaldt, M. Caravati, A. Baiker, *J. Phys. Chem. B* **2006**, *110*, 25586-25589
[34] A. F. Lee, K. Wilson, *Green Chem.* **2004**, *6*, 37-42
[35] D. Ferri, C. Mondelli, F. Krumeich, A. Baiker, *J. Phys. Chem. B* **2006**, *110*, 22982-22986.
[36] C. Keresszegi, D. Ferri, T. Mallat, A. Baiker, *J. Catal.* **2005**, *234*, 64-75.
[37] C. Keresszegi, D. Ferri, T. Mallat, A. Baiker, *J. Phys. Chem. B* **2005**, *109*, 958-967.
[38] A. Villa, D. Ferri, S. Campisi, C. E. Chan-Thaw, Y. Lu, O. Kröcher, L. Prati, *ChemCatChem* **2015**, *7*, 2534-2541.
[39] P. A. Christensen, S. W. M. Jones, A. Hamnett, *Phys. Chem. Chem. Phys.* **2013**, *15*, 17268-17276.
[40] E. A. Monyoncho, S. N. Steinmann, C. Michel, E. A. Baranova, T. K. Woo, P. Sautet, *ACS Catal.* **2016**, *6*, 4894-4906.
[41] Y.-Y. Yang, J. Ren, Q.-X. Li, Z.-Y. Zhou, S.-G. Sun, W.-B. Cai, *ACS Catal.* **2014**, *4*, 798-803.
[42] Z.-Y. Zhou, Q. Wang, J.-L. Lin, N. Tian, S.-G. Sun, *Electrochim. Acta* **2010**, *55*, 7995-7999.
[43] E. Groppo, G. Agostini, A. Piovano, N. B. Muddada, G. Leofanti, R. Pellegrini, G. Portale, A. Longo, C. Lamberti, *J. Catal.* **2012**, *287*, 44-54.
[44] G. Agostini, E. Groppo, A. Piovano, R. Pellegrini, G. Leofanti, C. Lamberti, *Langmuir* **2010**, *26*, 11204-11211.
[45] A. M. Bradshaw, F. M. Hoffmann, *Surf. Sci.* **1978**, *72*, 513-535.
[46] A. Ortega, F. M. Huffman, A. M. Bradshaw, *Surf. Sci.* **1982**, *119*, 79-94.
[47] E. Groppo, S. Bertarione, F. Rotunno, G. Agostini, D. Scarano, R. Pellegrini, G. Leofanti, A. Zecchina, C. Lamberti, *J. Phys. Chem. C* **2007**, *111*, 7021-7028.
[48] I. V. Yudanov, R. Sahnoun, K. M. Neyman, N. Rösch, J. Hoffmann, S. Schauermann, V. Johánek, H. Unterhalt, G. Rupprechter, J. Libuda, H.-J. Freund, *J. Phys. Chem. B* **2003**, *107*, 255-264.
[49] N. W. Alcock, V. M. Tracy, T. C. Waddington, *J. Chem. Soc., Dalton Trans.* **1976**, 2243-2246.
[50] D. Rivera, P. E. Poston, R. H. Uibel, J. M. Harris, *Anal. Chem.* **2000**, *72*, 1543-1554.
[51] H. Idriss, E. G. Seebauer, *J. Mol. Catal. Chem.* **2000**, *152*, 201-212.
[52] T. Moriyoshi, Y. Uosaki, K. Takahashi, T. Yamakawa, *J. Chem. Thermodyn.* **1991**, *23*, 37-42
[53] G. Agostini, R. Pellegrini, G. Leofanti, L. Bertinetti, S. Bertarione, E. Groppo, A. Zecchina, C. Lamberti, *J. Phys. Chem. C* **2009**, *113*, 10485-10492.
[54] R. Pellegrini, G. Leofanti, G. Agostini, L. Bertinetti, S. Bertarione, E. Groppo, A. Zecchina, C. Lamberti, *J. Catal.* **2009**, *267*, 40-49.

Entry for the Table of Contents

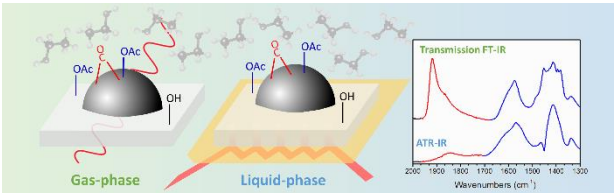

The interaction of gaseous as well as liquid ethanol over Pd/Al_2O_3 catalysts was studied by FT-IR and ATR-IR spectroscopies, respectively. We identified acetates and carbonyls as decomposition products and potential surface poisoning. Particular care is devoted to the rationalization of the catalysts properties affecting such phenomenon. This would allow for the design of systems able to minimize the unwanted poisoning.